Phys Chem Minerals (2011) 38:701–708
DOI 10.1007/s00269-011-0443-2

ORIGINAL PAPER

# Mössbauer hyperfine parameters of iron species in the course of *Geobacter*-mediated magnetite mineralization

**Yi-Liang Li · San-Yuan Zhu · Kun Deng**

Received: 24 March 2011 / Accepted: 28 May 2011 / Published online: 12 June 2011


**Abstract** Amorphous ferric iron species (ferrihydrite or akaganeite of <5 nm in size) is the only known solid ferric iron oxide that can be reductively transformed by dissimilatory iron-reducing bacteria to magnetite completely. The lepidocrocite crystallite can be transformed into magnetite in the presence of abiotic Fe(II) at elevated pH or biogenic Fe(II) with particular growth conditions. The reduction of lepidocrocite by dissimilatory iron-reducing bacteria has been widely investigated showing varying results. Vali et al. (Proc Natl Acad Sci USA 101:16121–16126, 2004) captured a unique biologically mediated mineralization pathway where the amorphous hydrous ferric oxide transformed to lepidocrocite was followed by the complete reduction of lepidocrocite to single-domain magnetite. Here, we report the $^{57}$Fe Mössbauer hyperfine parameters of the time-course samples reported in Vali et al. (Proc Natl Acad Sci USA 101:16121–16126, 2004). Both the quadrupole splittings and linewidths of Fe(III) ions decrease consistently with the change of aqueous Fe(II) and transformations of mineral phases, showing the Fe(II)-mediated gradual regulation of the distorted coordination polyhedrons of $Fe^{3+}$ during the biomineralization process. The aqueous Fe(II) catalyzes the transformations of Fe(III) minerals but does not enter the mineral structures until the mineralization of magnetite. The simulated abiotic reaction between Fe(II) and lepidocrocite in pH-buffered, anaerobic media shows the simultaneous formation of green rust and its gradual transformation to magnetite plus a small fraction of goethite. We suggested that the dynamics of Fe(II) supply is a critical factor for the mineral transformation in the dissimilatory iron-reducing cultures.

**Keywords** Mössbauer spectroscopy · Lepidocrocite · Green rust · Magnetite · Biomineralization · Iron-reducing bacteria

Y.-L. Li (✉) · S.-Y. Zhu
Department of Earth Sciences, The University of Hong Kong, Pok Fu Lam, Hong Kong
e-mail: yiliang@hku.hk

K. Deng
State Key Laboratory of Oil and Gas Reservoir Geology and Exploitation, Chengdu University of Technology, Chengdu, China

## Introduction

Hydrous ferric oxide (HFO or ferrihydrite) is an amorphous oxyhydroxide that can be reductively transformed to magnetite by the metabolism of dissimilatory iron-reducing bacteria (DIRB) as the end product. Though there are many ferric iron minerals being tested for potentially serving as electron acceptors for the respiration of DIRB (e.g., Roden and Zachara 1996; Zachara et al. 1998), lepidocrocite (LPD) is so far the only iron oxide, which has a well-crystallized form, that can be completely transformed to magnetite mediated by DIRB (Vali et al. 2004; O'Loughlin et al. 2010; Zegeye et al. 2010). Most crystallized Fe(III)-oxides are not preferred electron acceptors for DIRB by showing low reduction rates (e.g., Roden and Zachara 1996; Roden and Urrutia 2002; Roden 2006), and the reductive products were usually ferro-carbonate or ferro-phosphate rather than magnetite because of the kinetic difficulty in supplying substantial amounts of both soluble $Fe^{2+}$ and $Fe^{3+}$ for the crystallization of magnetite (Zachara et al. 1998; Dong et al. 2000).

Chemically, LPD crystallites can be transformed into magnetite by reacting with Fe(II) via a dissolution–recrystallization mechanism in the anoxic environments

(Cornell and Schwertmann 1996). However, the biological reduction of LPD was recently paid more attention due to the varied culturing-dependent mineralization pathways. Some studies demonstrated that crystalline LPD could not be used effectively by DIRB as electron acceptor to support their growth (Roden and Zachara 1996; Ona-Nguema et al. 2002; Glasauer et al. 2003; O'Loughlin et al. 2007). Some studies demonstrated that DIRB can only reduce LPD to green rust (GR) (Ona-Nguema et al. 2002; O'Loughlin et al. 2007), though GR could turn to magnetite upon the variation of temperature (Chaudhuri et al. 2001; Ona-Nguema et al. 2002). Recent studies indicated that the ratio of DIRB cell to LPD besides the kinetics of producing Fe(II) might determine the feature of cell–LPD aggregates and the final products to be GR or magnetite (O'Loughlin et al. 2010; Zegeye et al. 2010). Vali et al. (2004) showed that the incubation of *Geobacter metallireducens* strain GS-15 with HFO as electron acceptor demonstrated a unique, two-step pathway: firstly, HFO amended as electron acceptor was transformed to well-crystallized LPD; secondly, LPD crystals completely transformed to single-domain magnetite. Though interesting, the evolution of the microenvironments of Fe-species in the typical DIRB-mediated Fe-colloidal system was not reported in Vali et al. (2004). Recent developments in this field require understanding the hyperfine environments of iron species all through the biomineralization pathways. It is worth reporting the detailed change of Fe-species of Vali et al. (2004) because it was so far the only process that involved three mineral species with distinct structures.

$^{57}$Fe Mössbauer spectroscopy (MS) has extremely high-energy resolution and is sensitive to the short-range interactions in iron-containing solids. This method provides electron density and symmetry information of oxides and the accurate distribution of iron ions on lattices and $Fe^{2+}$/$Fe^{3+}$ ratio in the bulk composition (Burns 1994). In this study, we report MS hyperfine parameters of Fe in the time-course biomineralization process previously reported by Vali et al. (2004). The abiotic crystallization of magnetite from the reaction between LPD and soluble Fe(II) under anaerobic conditions was also examined for comparison.

## Experiments

### Preparation and characterization of HFO, LPD, and magnetite produced from LPD plus Fe(II) reaction

Preparation of HFO and identification of mineral phases in the culture of *Geobacter metallireducens* GS-15 can be partially found in the study by (Vali et al. 2004). For the abiotic simulation, LPD for this study was synthesized according to (Cornell and Schwertmann 1996). LPD was added to HEPES (Na-salt of 4-(2-hydroxyethyl)-1-piperazineethanesulfonic acid)-buffered anaerobic media (pH = 7.2) to bring the concentration of Fe(III) to ~60 mM. The media used to prepare GR did not contain sulfate or carbonate with $N_2$ of high purity as the headspace gas. For the preparation of magnetite from GR, Fe(II) stock solution was injected to LPD-containing media at room temperature to produce GR with Fe(II):Fe(III) ratios equal to 0.7:2, 1:2, and 1.3:2. The minerals in the reaction media were characterized by Tecnai G2 20 S-TWIN scanning transmission electron microscopy (STEM) in Hong Kong University.

### Reduction of HFO by GS-15

GS-15 was initially cultured using ferric citrate as the electron acceptor and acetate as the electron donor. The biomass was harvested after being incubated at 30°C in the dark to the exponential stage, washed by oxygen-free, deionized distilled water to remove iron, and re-dispensed to new anaerobic media to get a Fe-free inoculum for cell inoculation. During bacterial iron reduction, 2–3 tubes were sacrificed at each checking point. The sacrificed tubes were measured for acid-extracted Fe(II) using the ferrozine method (Stookey 1970) and their solid precipitates were measured for $^{57}$Fe Mössbauer spectra. Experiments were replicated with the same condition as used in Vali et al. (2004) many times but only yielded superparamagnetic magnetite as reported elsewhere (e.g., Sparks et al. 1990; Li et al. 2009).

### Powder X-ray diffraction and calculation of accurate lattice constant

Magnetite crystallites were scanned from 15° to 70° for $2\theta$ with a step of 0.02° per second by a Siemens D5000 X-ray diffractometer. Displacements were calibrated for small sample effects. The refined powder X-ray diffraction (pXRD) profiles were used to calculate $2\theta$ and $d$ values that were further used to extrapolate the accurate lattice constant of magnetite by the Nelson and Riley function (1945). The calculated $2\theta$ values with $\delta \geq 0.03^{\circ}$ and $d$ values with $\delta \geq 0.002$ Å were excluded for Nelson and Riley extrapolation. In this method, all valid crystallographic (hkl) values versus Neslon–Riley functions were used to extrapolate the lattice constant of $2\theta$ equal to 90°, which eliminates errors propagated from the instrumental measurements of $2\theta$ values.

### Mössbauer spectroscopy

Room-temperature Mössbauer spectra were collected at the Institute for Rock Magnetism, University of Minnesota.

Each 10-mg freeze-dried sample was sealed by Kapton tape in a Teflon ring of 1 $cm^2$ diameter. Spectra were recorded using a 50-mCi $^{57}Co$ source diffused in the rhodium film, moving in a constant acceleration mode with a symmetric double-ramp wave form. Spectra were folded to eliminate the parabolic background before fitting. The velocity scale was calibrated with reference to the spectrum of α-Fe foil. Highly purified helium gas was flushed during the resonance absorption to avoid oxidation of Fe(II) in the sample. The spectra containing sextets were fitted by using the early version of RECOIL (Rancourt and Ping 1991) with Voigt model of peak distribution. No constraints were applied to the relative sextet peak areas of magnetite and linewidth. For those Mössbauer profiles consisting of only one set of doublet, using Lorentian- or Voigt model did not show any difference. The recoilless fractions of iron in octahedral and tetrahedral crystallographic sites were considered equal (Gorski and Scherer 2010) for calculating the areas of subspectra. The set of hyperfine parameters was accepted by the result with the smallest least-square value and reasonable linewidths.

## Results

### Changing of colors of FHO-containing media induced by biogenic and abiotic Fe(II)

In the GS-15 culture with HFO as electron acceptor, the initial dark brown color of HFO slurry turned to ocher after 60 h of incubation. After 90 h of incubation, tiny black aggregates that were attracted to a magnet began to appear, indicating the formation of magnetite. After 125 h of incubation, more black aggregates could be observed at the bottom of the culturing tubes. The ocher color faded completely after 180 h of incubation and the culture slurry became clear. The 581- and 668-h samples showed stable existence of magnetite crystals. In the abiotic simulation, the injection of Fe(II) to the anaerobic LPD slurry simultaneously produced celadon-like green colored slurry of GR, which turned to magnetite plus minor goethite after about 12 h aging.

### Acid-extracted Fe(II) of the time-course samples

The 0.5 M HCl-extracted Fe(II) concentrations coincided with the sequence of color change and mineral transformations (Fig. 1). The decrease in Fe(II) at 24 h (0.44 mM) implies that the biogenic Fe(II) in the solution might be adsorbed to HFO or biomass (Roden and Zachara 1996; Liu et al. 2001). Following relatively constant Fe(II) values (3.16–3.22 mM) between 60- and 120-h incubation, a significant increase in acid-extracted Fe(II) occurred at

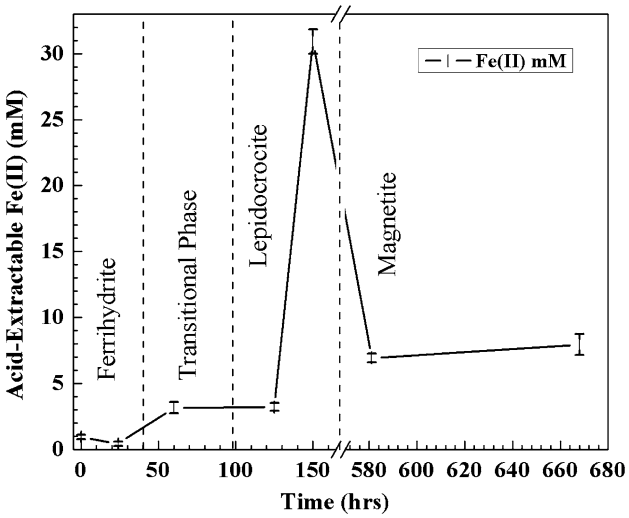


**Fig. 1** Time-series variation of acid-extracted Fe(II) concentrations. *Vertical dashed lines* demarcate time intervals over which a particular Fe-bearing phase dominates

150 h (30.92 mM) with a rapid increasing rate (1 mM/hr), which was consistent with the conspicuous transformation of γ-FeOOH to magnetite at this time. The concentration of Fe(II) decreased after 150 h and remained relatively constant between 581 h (6.94 mM) and 668 h (7.94 mM) (Fig. 1).

### Mössbauer hyperfine parameters

The MS results (Table 1; Fig. 2) substantiated the results of pXRD (Vali et al. 2004) and acid-extracted Fe(II) (Fig. 1). Spectra of 0 h (Fig. 2a) and 24 h (Fig. 2b) showed quadrupole doublets with the hyperfine parameters (IS = 0.35 mm/s, QS = 0.70 mm/s) similar to typical HFO (e.g., Cornell and Schwertmann 1996; Mitov et al. 2002; Kukkadapu et al. 2003). The spectrum of 60 h (Fig. 2c) appeared similar to the previous spectra; however, QS of $Fe^{3+}$ (0.63 mm/s) changed substantially and indicated the transformation toward γ-FeOOH (Fig. 1). Both spectra of 125 h (Fig. 2d) and 150 h (Fig. 2e) appeared to be weak sextets superimposed on strong quadrupole doublets. The sextets, characteristic of magnetic-ordered iron oxide, were too weak to be fitted for hyperfine parameters. The quadrupole doublets at 125–150 h (IS = 0.35 mm/s, QS = 0.55 mm/s) were the same as those of reported γ-FeOOH (McCammon 1995; Mitov et al. 2002; Ona-Nguema et al. 2002) and were clearly distinct from the parameters of goethite (Kondoro 1999; Kuzmann et al. 1998) or akageneite (Kuzmann et al. 1998). The 581-h (Fig. 2f) and 668-h (Fig. 2g) spectra were made of two sets of sextets of typical magnetite (McCammon 1995; Vandenberghe et al. 2000). The hyperfine fields of 489 kOe (581 h) and 490 kOe (668 h)

**Table 1** Mössbauer spectroscopic hyperfine parameters of time-course samples and magnetite plus goethite produced from the reaction between LPD and Fe(II) under anaerobic condition

| Time (h) | IS (mm/s) | QS (mm/s) | Area (%) | HWH (mm/s) | Hyperfine fields (kOe) | Phase |
|---|---|---|---|---|---|---|
| 0 | 0.35 | 0.70 | 100 | 0.26 | | Ferrihydrite |
| 24 | 0.35 | 0.70 | 100 | 0.26 | | Ferrihydrite |
| 60 | 0.34 | 0.63 | 100 | 0.22 | | Intermediate |
| 125 | 0.35 | 0.55 | 100 | 0.17 | | Lepidocrocite |
| 150 | 0.35 | 0.55 | 100 | 0.17 | | Lepidocrocite |
| 581 | 0.26 | −0.01 | 32.9 | 0.14 | 489 | Magnetite |
| | 0.63 | −0.02 | 67.1 | 0.29 | 458 | |
| 668 | 0.26 | 0.00 | 33.1 | 0.14 | 490 | Magnetite |
| | 0.63 | 0.00 | 66.9 | 0.29 | 458 | |
| Magnetite from reaction between LPD and Fe(II) | 0.29 | 0.00 | 33.3 | 0.21 | 473 | Magnetite |
| | 0.59 | 0.00 | 39.0 | 0.32 | 449 | |
| | 0.34 | −0.30 | 27.7 | 0.19 | 349 | Goethite |

*IS* isomer shifts, *QS* quadruple splitting, *HWH* half-width half-height of the peak

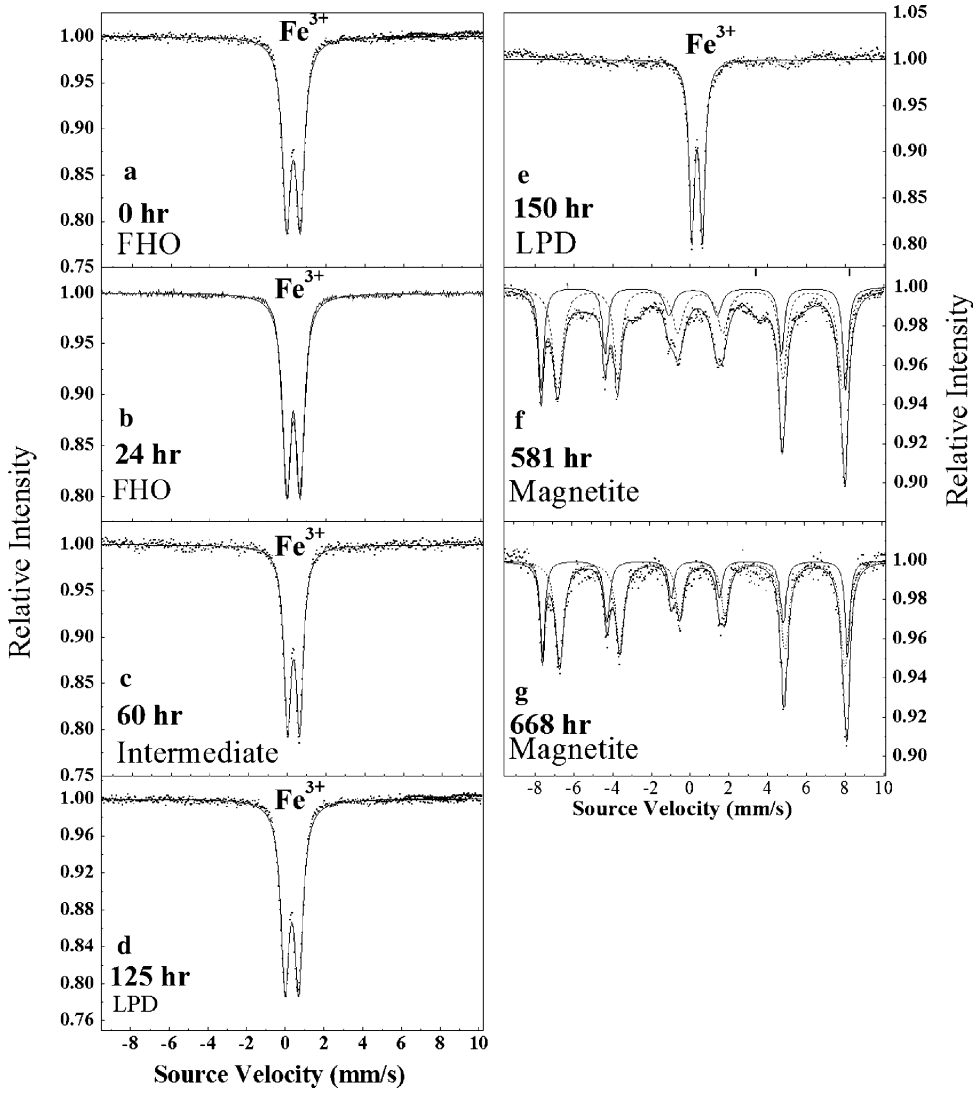


**Fig. 2** The time-course variation of the Mössbauer spectra of iron oxides during the incubation of GS-15

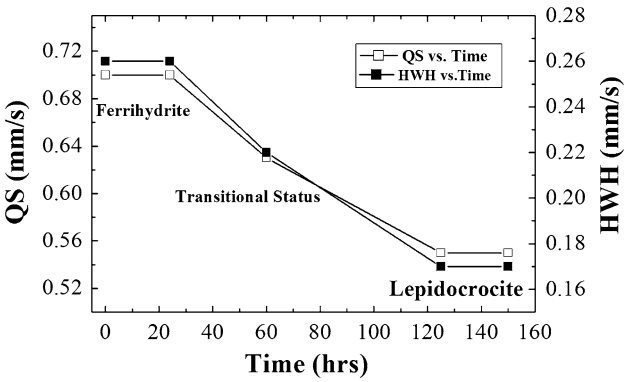


**Fig. 3** The relationship between mineral transformation and the evolution of hyperfine parameter quadrupole splitting (*QS*) and linewidth (HWH) as the function of time

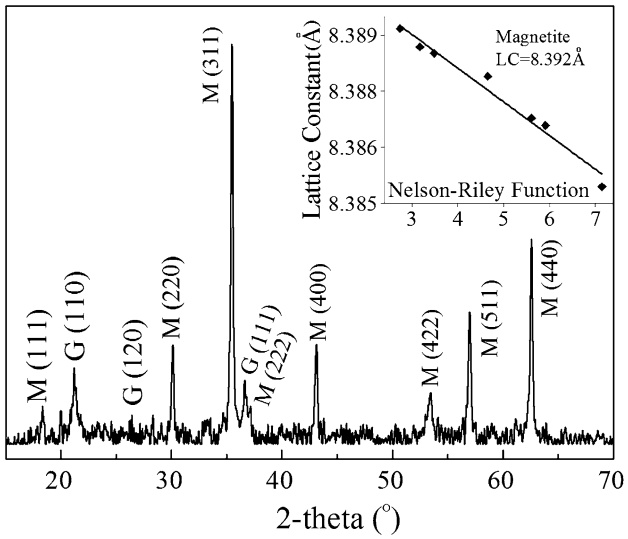


**Fig. 4** The pXRD profile of magnetite plus goethite produced from lepidocrocite plus Fe(II) reaction and the calculation of lattice constant of magnetite (*inset*). The *inset* shows the accurate lattice constant of magnetite calculated from the Nelson–Riley extrapolation method (Nelson and Riley 1946). *M* magnetite, *G* goethite

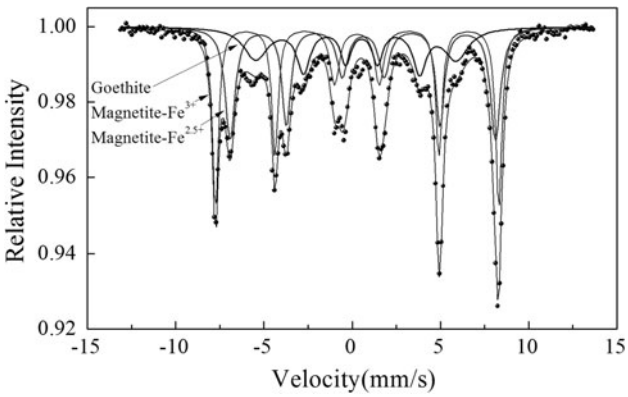


**Fig. 5** The Mössbauer spectroscopy of the final products of the interaction between lepidocrocite and Fe(II) under anaerobic condition showing the formation of magnetite and magnetically ordered goethite

(Table 1) represented $Fe^{3+}$ in the tetrahedral sites of magnetite; the hyperfine fields of 458 kOe (581 h) and 458 kOe (668 h) (Table 1) represented $Fe^{2.5+}$ in the octahedral sites of magnetite. The B:A ratio of the fitted area of magnetite $[(Fe^{3+})^{A}[Fe^{3+}Fe^{2+}]^{B}O_4]$ was slightly greater than 1.9:1, indicating a slight $Fe^{2+}$-excess (Vandenberghe et al. 2000; Li et al. 2009). The stoichiometry of the biogenic magnetite was calculated according to Gorski and Scherer (2010) to be $Fe_{2.997}O_4$.

The decreases in QS and linewidth of Fe(III) during the course of incubation were significant (Table 1; Fig. 3). The QSs and linewidths of $Fe^{3+}$ decreased from 0.7 and 0.26 mm/s in ferrihydrite to 0.55 and 0.17 mm/s in LPD. The hyperfine parameters of LPD at 150 h were exactly the same as those of 125 h, which indicated that the existence of LPD was a stable phase during this period. The MS spectra of abiotic simulations showed two sets of sextets for typical magnetite and a set of small sextet characterized of goethite (Table 1; Fig. 5).

## Crystallography of magnetite precipitated by abiotic simulation and GS-15 respiration

The pXRD (Fig. 4) and MS (Fig. 5) measurements of the end product of LPD plus soluble Fe(II) indicated the formation of magnetite plus a minor fraction of goethite. The LCs of magnetite crystals synthesized at room temperature with 0.7:2, 1:2, and 1.3:2 of Fe(II)/Fe(III) were 8.392, 8.394, and 8.392 Å. The LC of magnetite produced by GS-15 through the regular pathway (e.g., Sparks et al. 1990) is 8.404 Å, which was close to the previously reported LC of biogenic magnetite crystals (Li et al. 2009). The biogenic magnetite crystallites, though may suffer slight oxidation, still had its LC greater than that of stoichiometric magnetite (8.3967 Å of $Fe_3O_4$) (Zhang and Satpathy 1991).

LPD crystallites prepared according to (Cornell and Schwertmann 1996) were wisker-like with an average long axis of 180 ± 48 nm (Fig. 6a). The GR crystals around 0.5 μm (Fig. 6b) could be observed coexisting with remained LPD and ultrafine particles (inset of Fig. 6b, <5 nm). GR slurry turned to magnetite plus minor goethite filaments (Fig. 6c) after about 12 h. The inset of Fig. 6c was the selected area electron diffraction (SAED) pattern of magnetite. The magnetite crystallized from LPD had particle sizes averaged at 54 ± 18 nm.

## Discussion

HFO and LPD all have short-range ordered $Fe^{3+}(O)_6$ or $FeO_3(OH)_3$ octahedra. The transformation of HFO to LPD

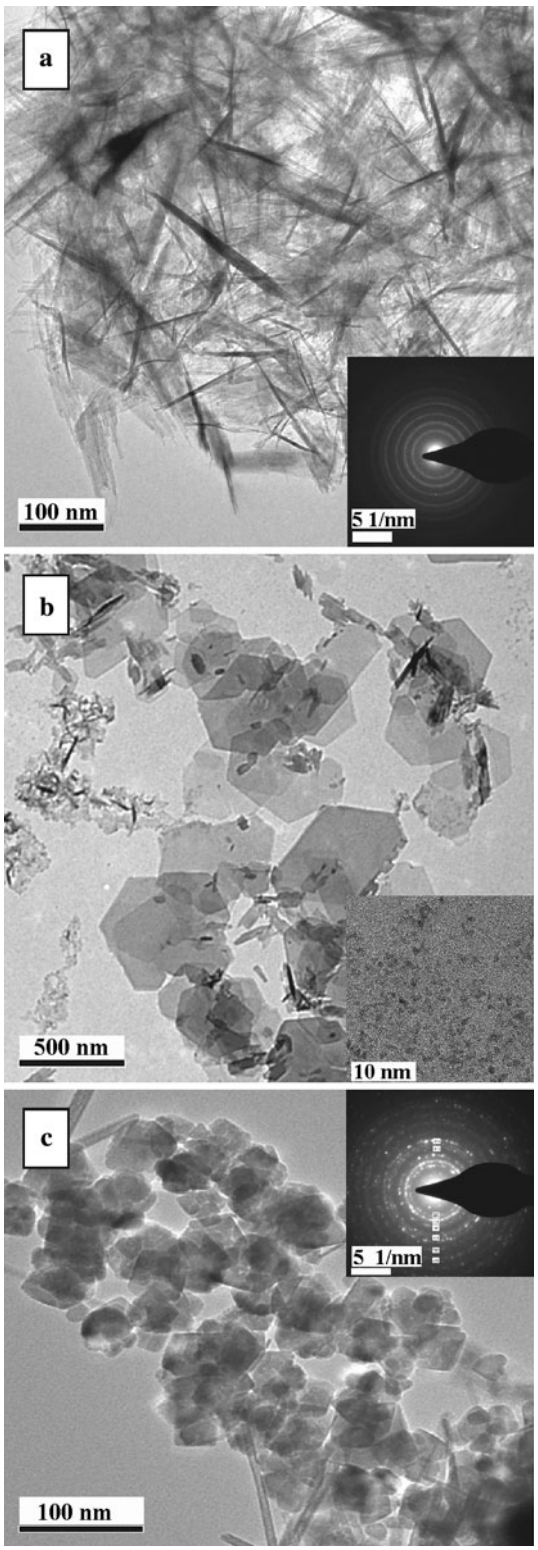


**Fig. 6** TEM characterization of hydrothermally synthesized lepidocrocite and its transformation to magnetite plus minor goethite by its reaction to Fe(II). **a**, *inset* shows lepidocrocite and its SEAD characterization; **b**, *inset* shows hexagonal green rust crystals and ultrafine particles (<5 nm) growing from the green rust slurry; **c**, *inset* shows the formation of magnetite plus goethite filaments as the final phases, and the SEAD characterization of magnetite

is a regulation of the highly distorted octahedra of HFO to octahedra of LPD with more symmetry that can be reflected by the decrease in QS (Mitra 1993). This hyperfine evolution of the microenvironments of Fe was clearly indicated by the decrease in QS and linewidth values (Fig. 3).

The transformation of HFO to $\gamma$-FeOOH is an uncommon pathway because HFO is unstable to goethite or hematite under aerobic conditions (e.g., Lindsay 1979; Schwertmann and Murad 1983; Delgado et al. 2003). If HFO is considered close to $Fe(OH)_3$ in stoichiometry, the biogenic Fe(II)-catalyzed transformation of HFO to LPD without redox reaction can be roughly expressed in this way:

$$Fe(OH)_3 + Fe(II) \rightarrow \gamma - FeOOH + Fe(OH)^- + H^+ \quad (1)$$

In the case of this study, the Fe(II)/ΣFe was around 5% at the early stage of incubation, which constrained the product to be LPD rather than magnetite or GR. After 120 h of incubation, the microbial production of Fe(II) (1 mM/h during 120–150 h, Fig. 1) was consistent with the "fast" Fe(II) production rate that led to the formation of magnetite (O'Loughlin et al. 2010). When there was enough LPD in the culture, high amount of Fe(II) was also accumulated (Fig. 1). The mineralization of magnetite from LPD could be described as follows:

$$2\gamma - FeOOH + Fe(OH)^- \rightarrow Fe_3O_4 + H_2O + H^+ \quad (2)$$

The production of proton may prohibit the crystallization of magnetite (e.g., Hansel et al. 2005) if the media were not pH buffered. As $Fe(OH)^-$ is soluble, it was never detected by MS all through the bacteria-mediated process (Fig. 2a–e) until the crystallization of magnetite (Fig. 2f, g).

Goethite can be one of the end products in the abiotic or biotic reduction of LPD toward the crystallization of magnetite (Figs. 4, 5, 6c; Hansel et al. 2003, 2004). In the abiotic simulations, massive GR crystals coexist with LPD relics, indicating that GR is an intermediate phase as the result of the dynamic dissolution of LPD by soluble Fe(II) (Ona-Nguema et al. 2002; Zegeye et al. 2010). The whole pathway can be summarized as follows:

$$\begin{aligned} &\gamma\text{-FeOOH} + Fe(II) + H_2O \\ &\rightarrow \left\{Fe^{II}_{(1-x)}Fe^{(III)}_{x}(OH)_2\right\}^{x+} \{(x/n)A^{n-}(m)H_2O\}^{x-}(GR) \\ &\rightarrow Fe_3O_4 + \alpha\text{-FeOOH} \end{aligned} \quad (3)$$

GR was not observed in the time-course samples of this study, which is characterized by having high-spin $Fe^{2+}$ (Ona-Nguema et al. 2002). We use undefined formula of GR (Eq. 3) rather than previously reported GR with better constrained composition (e.g., Ona-Nguema et al. 2002)

because the media we used to make GR did not contain any sulfate or carbonate that was found commonly in the formula of GR.

MS hyperfine parameters indicated that iron cations on lattices were paramagnetic high-spin $Fe^{3+}$ bonded to O- or OH-ligands before the nucleation of magnetite. The change of QS values and linewidths of Fe(III) ions of time-course samples indicated a gradual regulation of the distorted octahedral site and increasing of cubic symmetry (Burns 1994) of $Fe^{3+}$-coordinations. The large QS values of HFO indicated that $Fe^{3+}$ ions occupy highly distorted octahedral coordinated sites (Fig. 3). Both QS and linewidth values decreased with time (Fig. 3), indicating the regulation of the iron octahedral sites toward the symmetric cubic polyhedral coordination, which is consistent with the transformation of amorphous HFO to the crystalized LPD. The QS of 60 h captured an intermediate phase between HFO and LPD, which is not a typical 6-line HFO (Kukkadapu et al. 2003) but a transition state between HFO and LPD. The MS measurements showed no hyperfine parameters of any Fe(II) before the crystallization of magnetite in the time-course samples, indicating that Fe(II) only catalyze the phase transformation but does not enter the lattice of these crystals. This process is different from the one with GR as the intermediate phase (Ona-Nguema et al. 2002; O'Loughlin et al. 2010) in which the high-spin doublets of $Fe^{2+}$ exist in the crystal of GR.

The lattice constant values of biogenic magnetite crystals are close or even larger than that of ideal magnetite with perfect stoichiometry $[Fe^{3+}(Fe^{2+}Fe^{3+}O_4]$ (Li et al. 2009; Moon et al. 2010; Fischer et al. 2011). The Mössbauer spectroscopic $Fe^{2+}/Fe^{3+}$ and pXRD calculated lattice constant of magnetite produced from GR and GS-15 were all perfectly on the fitted linear equation of $Fe^{2+}/Fe^{3+}$ versus lattice constant of magnetite by Gorski and Scherer (2010) and in the domain of biogenic magnetite (Li et al. 2011). According to the linear equation of Gorski and Scherer (2010), the lattice constant of magnetite from GS-15 culture (8.404 Å) corresponds to a $Fe^{2+}/Fe^{3+}$ of 0.56, which is close to 0.53 calculated from the Mössbauer spectroscopic result. As both accurately measured $Fe^{2+}/Fe^{3+}$ by Mössbauer spectroscopy and lattice constant by pXRD are reliable for accurate stoichiometry of magnetite (Li et al. 2009, 2011; Gorski and Scherer 2010), the differences of $Fe^{2+}/Fe^{3+}$ and lattice constant of magnetite from the GS-15 culture and those from the transformation of GR were small but distinctable. The comparison indicated even with the similar processes that the abiotic magnetite is still different from the biogenic ones. Being produced at the same temperature, the crystal size of magnetite crystallized from GR (54 nm, Fig. 6c) was much smaller than the ~100-nm single-domain magnetite in the culture of GS-15 (Vali et al. 2004), but much larger than the superparamagnetic magnetite regularly produced in mesophilic DIRB cultures (Zachara et al. 1998; Li et al. 2009), implying the microbial mediation is still one of the important factors that controls the mineralization of magnetite.

**Acknowledgments** We thank Drs Mike Jackson, Peter Solheid, Bruce Moskowitz, Qingsong Liu and Brian Carter-Stiglitz for their kind help in experiments. Mössbauer spectroscopic measurements were supported by the National Science Grant of the United States and the Institute for Rock Magnetism, University of Minnesota. *Geobacter metallireducens* strain GS-15 was kindly provided by John Coates of the University of California, Berkeley. This study is supported by the State Key Laboratory of Oil and Gas Reservoir Geology & Exploitation (PLC200903).



## References

Burns RG (1994) Mineral Mössbauer spectroscopy: correlations between chemical shift and quadrupole splitting parameters. Hyper Interact 91:739–745

Chaudhuri SK, Lack JG, Coates JD (2001) Biogenic magnetite formation through anaerobic biooxidation Fe(II). Appl Environ Microbiol 67:2844–2848

Cornell RM, Schwertmann U (1996) The iron oxides. VCH, Weinheim, p 573

Delgado E, Bohórquez A, Pérez-Alcázar G, Bolanos A (2003) Study of the evolution in the iron oxide synthesis by hydrothermal process. Hyper Interact 148(149):129–134

Dong H, Fredrickson JK, Kennedy DW, Zachara JM, Kukkadapu RK, Onstott TC (2000) Mineral transformations associate with the microbial reduction of magnetite. Chem Geol 169:299–318

Fischer A, Schmitz M, Aichmayer B, Fratzl P, Faivre D (2011) Structural purity of magnetite nanoparticles in magnetotactic bacteria. J R Soc Interface, doi:10.1098/rsif.2010.0576

Glasauer S, Weidler PG, Langley S, Beveridge TJ (2003) Controls on Fe reduction and mineral formation by a subsurface bacterium. Geochim Cosmochim Acta 67:1277–1288

Gorski CA, Scherer MM (2010) Determination of nanoparticulate magnetite stoichiometry by Mössbauer spectroscopy, acidic dissolution, and powder X-ray diffraction: a critical review. Am Miner 95:1017–1026

Hansel CM, Benner SG, Neiss J, Dohnalkova A, Kukkadapu RK, Fendorf S (2003) Secondary mineralization pathways induced by dissimilatory iron reduction of ferrihydrite under advective flow. Geochem Cosmochim Acta 67:2977–2992

Hansel CM, Benner SG, Nico P, Fendorf S (2004) Structural constrains of ferric (hydr)oxides on dissimilatory iron reduction and the fate of Fe(II). Geochim Cosmochim Acta 68:3217–3229

Hansel CM, Benner SG, Fendorf S (2005) Competing Fe(II)-induced mineralization pathways of ferrihydrite. Environ Sci Technol 39:7147–7153

Kondoro JWA (1999) Mössbauer study of natural iron-oxide complexes. Hyper Interact 120(121):535–538

Kukkadapu RK, Zachara JM, Fredrickson JK, Smith SC, Dohnalkova AC, Russell CK (2003) Transformation of 2-line ferrihydrite to 6-line ferrihydrite under oxic and anoxic conditions. Am Miner 88:1903–1914

Kuzmann E, Nagy S, Vértes A, Weiszburg TG, Garg VK (1998) In: Vértes A, Nagy S, Süvegh K (eds) Nuclear methods in mineralogy and geology: techniques and applications. Plenum Press, New York, pp 285–376

Li YL, Pfiffner SM, Dyar M, Vali H, Konhauser K, Cole DR, Rondinone AJ, Phelps TJ (2009) Degeneration of biogenic superparamagentic magnetite. Geobiology 7:25–34

Li YL, Konhauser KO, Cole DR, Phelps TJ (2011) Mineral ecophysiological data provides growing evidence for microbial activity in banded-iron formation. Geology, doi:10.1130/G32003.1

Lindsay W (1979) Chemical equilibrium in soils. Wiley, New York, p 449

Liu C, Zachara JM, Gorby YA, Szecsody JE, Brown CF (2001) Microbial reduction of Fe(III) and sorption/precipitation of Fe(II) on *Shewanella putrefaciens* strain CN32. Environ Sci Technol 35:1385–1393

McCammon CA (1995) Mössbauer spectroscopy of minerals. In: Ahrens TJ (ed) Mineral physics and crystallography: a handbook of physical constants. AGU Ref. Shelf 2, pp 332–347

Mitov I, Paneva D, Kunev B (2002) Comparative study of the thermal decomposition of iron oxyhydroxides. Thermochim Acta 386:179–188

Mitra S (1993) Applied Mössbauer spectroscopy: theory and practice for geochemists and archeologists. Pergamon Press, Oxford

Moon J-W, Rawn CJ, Rondinone AJ, Wang W, Vali H, Yeary LW, Love LJ, Kirkham MJ, Gu B, Phelps TJ (2010) Crystallite size and lattice parameters of nano-biomagnetite particles. J Nanosci Nanotech 10:8298–8306

Nelson JB, Riley DP (1945) An experimental investigation of extrapolation methods in the derivation of accurate unit-cell dimensions of crystals. Proc Phys Soc 57:160–177

O'Loughlin EJ, Larese-Casanova P, Scherer M, Cook R (2007) Green rust formation from the bioreduction of $\gamma$-FeOOH (lepidocrocite): comparison of several *Shewanella* species. Geomicrobiol J 24:211–230

O'Loughlin EJ, Gorski CA, Scherer MM, Boyanov MI, Kemner KM (2010) Effects of oxyanions, natural organic matter, and bacterial cell numbers on the bioreduction of lepidocrocite (gamma-FeOOH) and the formation of secondary mineralization products. Environ Sci Technol 44:4570–4576

Ona-Nguema G, Abdelmoula M, Jorand F, Benali O, Géhin A, Block J-C, Génin J-MR (2002) Iron(II, III) hydroxycarbonate green rust formation and stabilization from lepidocrocite bioreduction. Environ Sci Technol 36:16–20

Rancourt DG, Ping JY (1991) Voigt-based methods for arbitrary-shape static hyperfine parameter distributions in Mössbauer spectroscopy. Nucl Instrum Methods Phys Res Sec B 58:85–97

Roden EE (2006) Geochemical and microbiological controls on dissimilatory iron reduction. C R Geosci 338:456–467

Roden EE, Urrutia MM (2002) Influence of biogenic Fe(II) on bacterial crystalline Fe(III) oxide reduction. Geomicrobiol J 19:209–251

Roden EE, Zachara JM (1996) Microbial reduction of crystalline Fe(III) oxides: influence of oxide surface area and potential for cell growth. Environ Sci Technol 30:1618–1628

Schwertmann U, Murad E (1983) Effect of pH on the formation of goethite and hematite from ferrihydrite. Clays Clay Miner 31:277–284

Sparks NHC, Mann S, Bazylinski DA, Lovley DR, Jannasch HW, Frankel RB (1990) Structure and morphology of magnetite anaerobically produced by a marine magnetotactic bacteria and a dissimilatory iron-reducing bacterium. Earth Planet Sci Lett 98:14–22

Stookey LL (1970) Ferrozine—a new spectrophotometric reagent for iron. Analyt Chem 42:779–781

Vali H, Weiss B, Li Y-L, Sears SK, Kim SS, Kirschvink JL, Zhang CL (2004) Formation of tabular single domain magnetite induced by *Geobacter metallireducens* GS-15. Proc Natl Acad Sci USA 101:16121–16126

Vandenberghe RE, Barrero CA, da Costa GM, Van San E, De Grave E (2000) Mössbauer characterization of iron oxides and (oxy)hydroxides: the present state of the art. Hyper Interact 126:247–259

Zachara JM, Fredrickson JK, Li S-M, Kennedy DW, Smith SC, Gassman PL (1998) Bacterial reduction of crystalline $Fe^{3+}$ oxides in single phase suspensions and subsurface materials. Am Miner 83:1426–1443

Zegeye A, Mustin C, Jorand F (2010) Bacterial and iron oxide aggregates mediate secondary iron mineral formation: green rust versus magnetite. Geobiology 8:209–222

Zhang Z, Satpathy S (1991) Electron states, magnetism, and the Verwey transition in magnetite. Phys Rev B44:13319–13331